Journal of Experimental Botany, Vol. 69, No. 16 pp. 4033–4045, 2018
doi:10.1093/jxb/ery188 Advance Access publication 18 May 2018
This paper is available online free of all access charges (see https://academic.oup.com/jxb/pages/openaccess for further details)

RESEARCH PAPER

Leaf hydraulic vulnerability triggers the decline in stomatal and mesophyll conductance during drought in rice

Xiaoxiao Wang[1,#] Tingting Du[1,#] Jianliang Huang[1], Shaobing Peng[1], and Dongliang Xiong[1,2,*]

[1] National Key Laboratory of Crop Genetic Improvement, MOA Key Laboratory of Crop Ecophysiology and Farming System in the Middle Reaches of the Yangtze River, College of Plant Science and Technology, Huazhong Agricultural University, Wuhan, Hubei 430070, China
[2] Department of Plant Sciences, University of California, Davis, CA 95616, USA

[#] These authors contributed equally to this work.
* Correspondence: dlxiong@mail.hzau.edu.cn or dlxiong@ucdavis.edu

Received 1 February 2018; Editorial decision 14 May 2018; Accepted 14 May 2018

Editor: Tracy Lawson, University of Essex, UK

Abstract

Understanding the physiological responses of crops to drought is important for ensuring sustained crop productivity under climate change, which is expected to exacerbate the frequency and intensity of periods of drought. Drought responses involve multiple traits, and the correlations between these traits are poorly understood. Using a variety of techniques, we estimated the changes in gas exchange, leaf hydraulic conductance, and leaf turgor in rice (*Oryza sativa*) in response to both short- and long-term soil drought. We performed a photosynthetic limitation analysis to quantify the contributions of each limiting factor to the resultant overall decrease in photosynthesis during drought. Biomass, leaf area, and leaf width significantly decreased during the 2-week drought treatment, but leaf mass per area and leaf vein density increased. Light-saturated photosynthetic rate declined dramatically during soil drought, mainly due to the decrease in stomatal conductance (g_s) and mesophyll conductance (g_m). Stomatal modeling suggested that the decline in leaf hydraulic conductance explained most of the decrease in stomatal closure during the drought treatment, and may also trigger the drought-related decrease of stomatal conductance and mesophyll conductance. The results of this study provide insight into the regulation of carbon assimilation under drought conditions.

Keywords: Drought, leaf hydraulic conductance, mesophyll conductance, photosynthesis limitation, rice, stomatal conductance, vulnerability.

Introduction

Plant productivity is significantly impacted by drought events, which are expected to occur more intensely and frequently as global climate change continues (Trenberth *et al.*, 2013). To develop new approaches to improve crop production under future conditions of water limitation, the responses of several physiological processes, including photosynthesis, plant hydraulic conductivity, and cell turgor pressure, have been widely documented (Flexas *et al.*, 2002; Grassi & Magnani, 2005; Flexas *et al.*, 2009; Galle *et al.*, 2011; Cano *et al.*, 2013; Galmés *et al.*, 2013; Rodriguez-Dominguez *et al.*, 2016; Gleason *et al.*, 2017; Martínez-Vilalta & Garcia-Forner, 2017); however, the correlations among these physiological traits have not been fully evaluated under drought conditions.

In C_3 plants, the light-saturated leaf photosynthetic rate (A) is limited by stomatal conductance (g_s), mesophyll conductance to CO_2 (g_m), and/or the photosynthetic biochemistry related to either carboxylation velocity, V_{cmax}, or the maximum electron transport rate set by photochemical and Calvin cycle activities, J_{max} (Tosens *et al.*, 2012; Tomás *et al.*, 2013; Tosens *et al.*, 2016; Veromann-Jürgenson *et al.*, 2017). Grassi and Magnani (2005)

developed a method to estimate the partial contribution of each limiting factor to the overall reduction of photosynthesis; this approach has since been applied to many species under a variety of environmental stresses (Flexas *et al.*, 2009; Galle *et al.*, 2009; Galle *et al.*, 2011; Galmés *et al.*, 2013; Wang *et al.*, 2018). Although the limiting effects of g_s, g_m, and photosynthetic biochemistry on A are dependent on the species, A has been suggested to be first inhibited by a decrease in g_s and g_m under drought conditions, with the biochemical inhibition occurring later, under more severe drought stress conditions (Grassi & Magnani, 2005; Flexas *et al.*, 2009; Galle *et al.*, 2009; Galle *et al.*, 2011; Galmés *et al.*, 2013; Galmés *et al.*, 2017). However, the contribution of each limiting factor to A under drought conditions, especially dynamic drought conditions, is unknown for rice (*Oryza sativa*), despite its status as one of the most important cereal crops in the world.

When plants are exposed to drought, their stomata close, preventing a decline in leaf water potential (ψ_{leaf}) and thereby ensuring that the water demand in leaves does not exceed the safe threshold of the hydraulic system (Scoffoni *et al.*, 2017*b*); however, the mechanisms underlying stomatal closure in response to soil drought are poorly understood. Both hormonal (Dodd, 2005) and leaf turgor (Sperry *et al.*, 2002; Buckley, 2005; Brodribb & Cochard, 2009; Rodriguez-Dominguez *et al.*, 2016) signals have been proposed to explain stomatal closure in angiosperms during drought conditions. The hormonal hypothesis suggests that stomatal closure in the leaves is principally driven by hormonal signals, especially abscisic acid (ABA) produced *de novo* in the leaf (Holbrook *et al.*, 2002; McAdam *et al.*, 2016; Zhang *et al.*, 2018). The leaf turgor hypothesis proposes that the decline in g_s during soil drought is caused by change in leaf turgor. Recently, a serial study (McAdam & Brodribb, 2016; McAdam *et al.*, 2016) tried to link these two hypotheses by demonstrating that, in response to low relative humidity, ABA is rapidly synthesized *de novo* and accumulates in the leaf once the leaf turgor declines in angiosperms. By contrast, a recent theoretical analysis suggested that ABA accumulation in dehydrated leaves is associated with a decline in cell volume, rather than a loss of turgor pressure (Sack *et al.*, 2018).

A decrease in g_m in response to soil drought was also observed in many previous studies, although the mechanisms for this decrease are unclear (Flexas *et al.*, 2002; Grassi & Magnani, 2005; Warren, 2008; Galle *et al.*, 2009; Cano *et al.*, 2013; Théroux-Rancourt *et al.*, 2014). Many studies have demonstrated the parallel responses of g_s and g_m to environmental changes (see review in Flexas *et al.*, 2012). The physiological basis of this relationship is largely unknown; however, recent studies in plant hydraulics suggest that leaf hydraulic conductance (K_{leaf}) mediates the covariation of g_s and g_m (Flexas *et al.*, 2013; Xiong *et al.*, 2015*b*; Xiong *et al.*, 2017; Xiong *et al.*, 2018). The liquid water transport pathways in the mesophyll are partially shared with the CO_2 diffusion pathways; hence, a functional linkage between g_m and K_{leaf} has been suggested. Similarly, g_s and K_{leaf} may be coupled because of the common stomatal pathway for the exchange of water and CO_2 between the leaf and the atmosphere. Correlations between K_{leaf} and g_s or g_m have been observed in many species and genotypes (Brodribb *et al.*, 2005; Brodribb *et al.*, 2007; Flexas *et al.*, 2013; Théroux-Rancourt *et al.*, 2015; Xiong *et al.*, 2018). Nonetheless, it is unclear whether a coordinated regulation of g_s, g_m, and K_{leaf} occurs under varied environmental conditions, for instance, during water stress. Indeed, K_{leaf} declines rapidly between full turgor and the turgor loss point and even more strongly during extreme dehydration (reviewed in Scoffoni *et al.*, 2017*b*). The response of K_{leaf} to dehydration has been suggested to arise mainly due to the vulnerability of tissues outside the xylem, such as mesophyll (Scoffoni *et al.*, 2017*a*), the major tissue where water transport and CO_2 diffusion may share a common pathway (Xiong *et al.*, 2017). Théroux-Rancourt *et al.* (2014) observed that K_{leaf} and g_s decreased as the soil water potential declined, but that g_m decreased only after g_s was <0.15 mol m^{-2} s^{-1} in poplars (*Populus* sp.). Revealing the regulatory patterns of these traits in response to drought is necessary for enhancing our understanding of plant responses to water limitation (Scoffoni *et al.*, 2017*b*).

In this study, we estimated gas exchange, K_{leaf}, and leaf turgor in response to both short- and long-term soil drought in two rice genotypes to reveal the correlations between and sequences of changes in these traits during the response to drought stress. The objectives of this study were (i) to reveal the dynamic limiting effects of g_s, g_m, and the photosynthetic biochemistry on A during drought in rice; and (ii) to clarify the vulnerabilities of A, g_s, g_m, and K_{leaf} and their relationships under drought conditions.

Materials and methods

Plant materials and growth conditions

Two 'Super' hybrid rice cultivars, Yangliangyou 6 (YLY6) and Chaoyou 1000 (CY1000), were used in this study. YLY6 is a widely used reference cultivar in promotion trials of newly developed 'Super' varieties in China, while CY1000 is a recently developed 'Super' variety with high yield and wide adaptation characteristics. Seeds were germinated and grown in a nursery for 2 weeks, and the seedlings were then transplanted into 11 litre plastic pots containing 10 kg of soil, at a density of three plants per pot. Before transplantation, 7.0 g of compound fertilizer ($N:P_2O_5:K_2O$=16:16:16%; Batian Ecological Engineering Limited, Shenzhen, China) was mixed into the soil of each pot. For each genotype, 60 randomly arranged pots of seedlings were grown, and pots were watered daily before the drought experiment began. Seven weeks after transplantation, 10 pots of each genotype were subjected to long-term water deficiency stress by maintaining a relative soil water content of ~75% for 2 weeks (Fig. 1A).

Gas exchange and chlorophyll fluorescence measurements

To avoid the effects of fluctuations in outdoor air temperatures, light intensity, and humidity (see Supplementary Fig. S1 at *JXB* online) on gas exchange, each measurement was taken between 09.00 h and 16.00 h in an environmentally controlled growth chamber (Model GR48; Conviron, Controlled Environments Limited, Winnipeg, MB, Canada), with an air temperature of 25 °C, a relative air humidity of 70%, and a photosynthetic photon flux density (PPFD) of 600 μmol m^{-2} s^{-1}. The night before the gas exchange measurements, the second fully expanded leaf of each plant was covered with both a plastic sheet and aluminum foil to estimate the stem water potential (ψ_{stem}) of the plant. After acclimating the plants overnight in the growth chamber, gas exchange measurements were carried out on the uppermost newly and fully expanded leaves, using a LI-6400 portable photosynthesis system equipped with a LI-6400–40 chamber (LI-COR Inc., Lincoln, NE, USA). In the leaf

chamber, the PPFD was maintained at 1500 μmol m^{-2} s^{-1}, the leaf-to-air vapor pressure deficit (VPD) was 1.5–2.0 kPa, and the CO_2 concentration was adjusted to 400 μmol mol^{-1} using a CO_2 mixer. The block temperature during the measurements was set to 25 °C. After stabilization to a steady state, the gas exchange parameters, steady-state fluorescence (F_s), and maximum fluorescence (F'_m) were recorded. The actual photochemical efficiency of photosystem II (Φ_{PSII}) was calculated as follows:

$$\Phi_{PSII} = \frac{(F'_m - F_s)}{F'_m} \quad (1)$$

The electron transport rates (J_f) were computed as follows:

$$J_f = \Phi_{PSII} \cdot PPFD \cdot \alpha \cdot \beta \quad (2)$$

where α is the leaf absorbance and β represents the distribution of electrons between photosystem I and photosystem II. After the gas exchange measurement, both ψ_{stem} and the leaf water potential (ψ_{leaf}) were determined using a pressure chamber (PMS Instrument Company, Albany, OR, USA) after equilibrating for at least 30 min.

To estimate α and β, light response curves for both well-watered and water-stressed plants were measured. The gas exchange system was switched to a low O_2 concentration (<2%) by injecting pure N_2, and simultaneous measurements of the light response curves and chlorophyll fluorescence were performed. During the measurements, the chamber conditions were the same as those described above, except that a gradient of PPFD values was used: 2000, 1500, 1200, 1000, 800, 600, 400, 200, 100, and 0 μmol m^{-2} s^{-1}. After reaching a steady state, the parameters of gas exchange and chlorophyll fluorescence were simultaneously recorded. The slope of the relationship between Φ_{PSII} and $4\Phi_{CO2}$ (the quantum efficiency of CO_2 uptake) was considered to represent the value of α·β (Valentini *et al.*, 1995). As there were no differences in the α·β values between the control and water-stressed leaves, the average value for all genotypes was used.

The mesophyll conductance of CO_2 (g_m) was calculated based on the variable *J* method described by Harley *et al.* (1992), as follows:

$$g_m = A / \left(C_i - \frac{\Gamma\star \left(J_f + 8\left(A + R_d\right)\right)}{J_f - 4\left(A + R_d\right)} \right) \quad (3)$$

where Γ⋆ represents the CO_2 compensation point in the absence of respiration, R_d is the day respiration rate, which was assumed to be half of the dark respiration rate (R_{dark}), C_i represents the intercellular CO_2 concentration, which was determined from an estimation of the cuticular conductance (see below) in this study, and C_c is the CO_2 concentration in the chloroplast. Γ⋆ is related to the Rubisco specific factor ($S_{C/O}$), which is relatively conserved at a given temperature. In the present study, the rice $S_{C/O}$ at 25 °C was obtained from Hermida-Carrera *et al.* (2016).

Cuticular conductance and C_i calibration

The method of Sack and Scoffoni (2011) was used to estimate the minimum leaf conductance (g_{cut}). The leaves were scanned using a Canon EOS M50 (Canon Inc., Tokyo, Japan) to calculate their area, and then dried in a room with an air temperature of 25.0 °C and a light intensity of <5 μmol m^{-2} s^{-1}. Leaves were weighed every 10 min over ~300 min using a digital balance (Sartorius BP 2215, Gottingen, Germany). The cuticular transpiration rate was determined from the regression of the change in leaf mass over time. Temperature and humidity sensors (HOB; H21-002; Onset Computer Corporation, Bourne, MA, USA) were placed next to the samples, and the air temperature and relative humidity were recorded

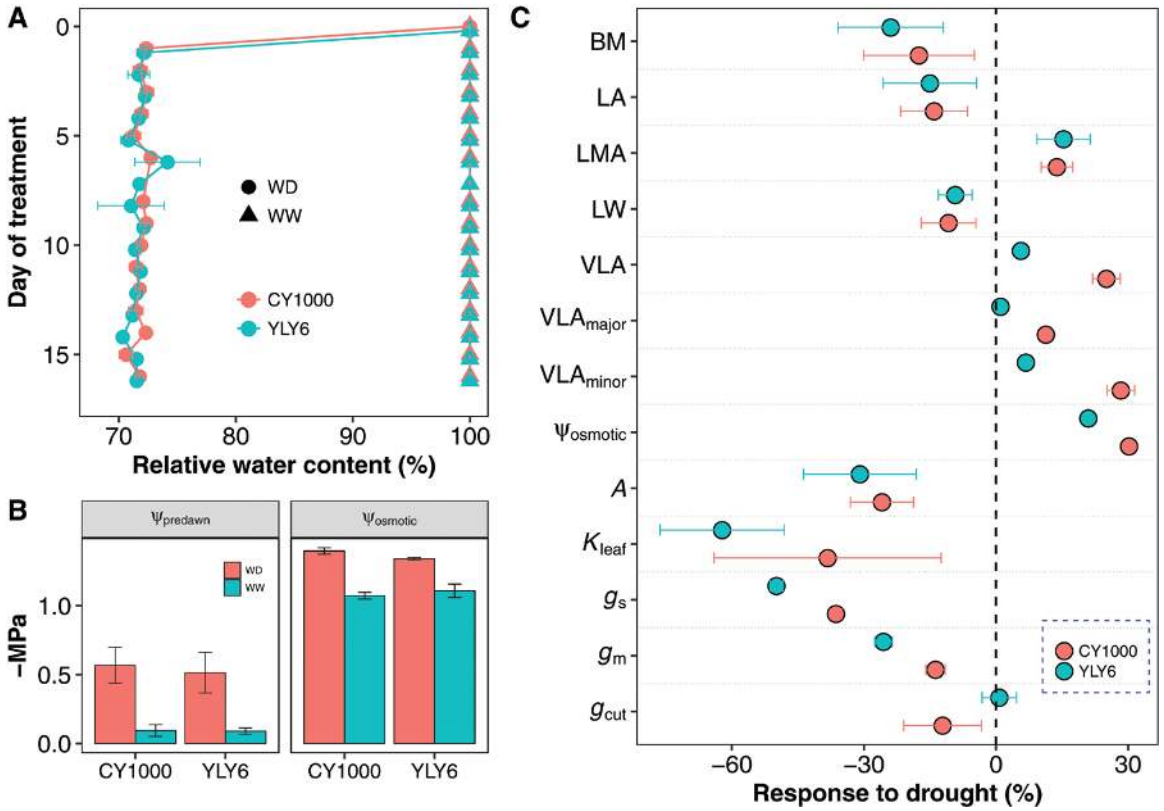

Fig. 1. (A) Soil relative water content of the well-watered (WW) and water-deficient (WD) treatments. (B) Predawn leaf water potential ($\psi_{predawn}$) and leaf osmotic potential ($\psi_{osmotic}$) of two rice genotypes after a 2-week drought treatment. See Supplementary Table S1 for definitions of the parameters. (C) Responses of leaf traits to 2 weeks of drought. The response was calculated as $\ln(X_{WD}/X_{WW})$, where X_{WD} and X_{WW} were mean values of trait *X* under the WD and WW treatments, respectively. (This figure is available in colour at *JXB* online.)

at the beginning of each weighing cycle to determine the VPD. The value of g_{cut} was calculated as the transpiration rate divided by the VPD.

It is a widely accepted norm that water vapor diffusing through stomata can be used to calculate the C_i; however, the calculations assume an identical gas phase path for CO_2 and water vapor, which does not hold under drought conditions. As stomata close, the cuticle becomes the dominant path of water vapor diffusion (Boyer *et al.*, 1997; Boyer, 2015*a*; Hanson *et al.*, 2016). Indeed, it has been suggested that C_i could potentially be overestimated, as the cuticular conductance is far greater for water than for CO_2 (Boyer, 2015*b*). Thus, in this study, we recalculated C_i to take g_{cut} into account, as follows:

$$C_i = \frac{(g_{sc} - E_s/2)\cdot C_{as} - A}{g_{sc} + E_s/2} \quad (4)$$

$$g_{sc} = (g_{lw} - g_{cut})/1.6 \quad (5)$$

$$E_s = E_l - g_{cut}(W_l - W_a) \quad (6)$$

where C_{as} is the CO_2 concentration at the leaf surface (400 μmol mol^{-1}), g_{sc} is the true stomatal conductance to CO_2, E_s is stomatal transpiration, g_{lw} is the total leaf conductance to water, E_l is leaf transpiration, and W_l and W_a are the water vapor values inside and outside the leaf, respectively.

Hydraulic vulnerability

Three methods were used to estimate K_{leaf}: the standard evaporative flux method (EFM), the rehydration kinetic method (RKM), and the gas exchange-based EFM method. The EFM was calculated following the methods outlined by Scoffoni *et al.* (2012) and Xiong *et al.* (2017). The rice tillers were bench-dried, and then the initial leaf water potential (ψ_0) was measured in the neighboring leaves. The dehydrated leaves were excised from the tillers under water and connected to a tube system, which was connected to a reservoir of degassed water situated on a high-precision digital balance (NBL 84e, Adam Equipment Inc., Oxford, UK). The balance logs data to a computer every 10 s. Once the water flow rate was stable (~30 min), the water flow rate (E) into the leaves under favorable conditions (on a large box fan with PPFD>1000 μmol m^{-2} s^{-1}) was recorded, along with the leaf temperature. Next, the leaf area (LA) and final leaf water potential (ψ_{final}) were measured. The $K_{leaf\text{-}EFM}$ was calculated as follows:

$$K_{leaf\text{-}EFM} = \frac{E}{LA\cdot(0-\psi_{final})} \quad (7)$$

The RKM was calculated following the method outlined by Blackman and Brodribb (2011). The ψ_0, leaf temperature, initial maximum rehydration flow of water into leaves (I), and LA were measured in a similar manner to the EFM method described above, except that the leaves were covered with moist paper and were not exposed to light, in order to prevent transpiration during the I measurement. I was calculated by fitting an exponential curve through the first 10 s of the flow data and extrapolating back to the initial point of leaf excision. $K_{leaf\text{-}RKM}$ was calculated as follows:

$$K_{leaf\text{-}RKM} = \frac{I}{LA\cdot\psi_0} \quad (8)$$

We also measured K_{leaf} using the transpiration rate (T_r) values from the gas exchange measurement and ψ_{stem}, and ψ_{leaf} after the gas exchange. For this method, $K_{leaf\text{-}licor}$ was calculated as follows:

$$K_{leaf\text{-}licor} = \frac{T_r}{\psi_{stem} - \psi_{leaf}} \quad (9)$$

To construct the vulnerability curve, K_{leaf} was plotted against the lowest ψ_{leaf} (i.e. ψ_0 in RKM; ψ_0 or ψ_{final} in EFM, and ψ_{leaf} in the gas exchange method). Because the viscosity of water is temperature dependent, the K_{leaf} values in this study were standardized to their corresponding value at 25 °C (Scoffoni *et al.*, 2012).

Pressure–volume curves

Four pressure–volume curves per genotype were conducted with well-watered plants, to estimate their osmotic potential at full turgor (π_0) and at the turgor loss point (π_{tlp}), as well as their modulus of elasticity (ε) (Sack *et al.*, 2003; Scoffoni *et al.*, 2011). Leaves were sampled from well-watered plants and rehydrated overnight before desiccation. Briefly, the leaf weight and ψ_{leaf} were measured at least 10 times over the desiccation period until ψ_{leaf} dropped to −3.0 MPa. Finally, the leaves were dried at 70 °C for 2 days and their dry mass was measured.

Osmotic potential measurements

The fully expanded young leaves of well-watered and water-stressed plants were sampled in the morning. The leaf samples were immersed in liquid nitrogen and then stored at −80 °C. The osmotic potentials of these leaves were measured using a vapor pressure osmometer (VAPRO 5520; Wescor Inc., Logan, UT, USA).

Leaf vein density

The newly developed and fully expanded leaves of both well-watered and water-stressed plants were chemically cleared in 15% NaOH (w/v) and then bleached following the standard protocol for rice (Xiong *et al.*, 2015*b*; Xiong *et al.*, 2017). The cleared leaves were stained with safranin and fast green in ethanol. After being rinsed in water, the leaves were scanned using a Canon EOS M50 (Canon Inc., Tokyo, Japan) to enable quantification of their area and major vein lengths. To measure the minor veins, a light microscope (U-TVO.5XC; Olympus, Tokyo, Japan) with a 5× objective was used to observe the leaves, and photographs were taken of the top, middle, and bottom of each leaf. LA and vein length were manually measured using ImageJ (Wayne Rasband/NIH, Bethesda, MD, USA). The total vein density (VLA), major vein density (VLA_{major}, including the midrib and large veins), and minor vein density (VLA_{minor}) were estimated.

Biomass and leaf area

Four plants per treatment were sampled after 2 weeks of drought treatment and were separated into stems and leaves. The LA was measured using a LA meter (LI-3100; LI-COR Inc., Lincoln, NE, USA). The samples were dried to a constant weight at 80 °C and their biomass was recorded.

Photosynthetic limitation analysis

A limitation analysis is a helpful tool for quantifying the effects of stress on various factors affecting A (Grassi & Magnani, 2005; Buckley & Diaz-Espejo, 2015). The relative photosynthetic limitations, including the relative stomatal (l_s), mesophyll (l_m), and biochemical (l_b) limiting effects, were modeled as previously described by Grassi and Magnani (2005):

$$l_s = \frac{g_t/g_{sc}\cdot\partial A/\partial C_c}{g_t + \partial A/\partial C_c} \quad (10)$$

$$l_m = \frac{g_t/g_m\cdot\partial A/\partial C_c}{g_t + \partial A/\partial C_c} \quad (11)$$

$$l_b = \frac{g_t}{g_t + \partial A/\partial C_c} \quad (12)$$

where g_t is the total conductance, which is calculated as:

$$g_t = \frac{1}{\frac{1}{g_{sc}} + \frac{1}{g_m}} \quad (13)$$

To assess the impact of ψ_{leaf} change on photosynthesis, the limiting effects were linked to overall changes in A:

$$\frac{dA}{A} = \text{LS+LM+LB} = \frac{dg_{sc}}{g_{sc}} l_s + \frac{dg_m}{g_m} l_m + \frac{dJ_f}{J_f} l_b \quad (14)$$

where LS, LM, and LB are the reduction fractional limitations in A caused by a reduction in stomatal conductance, mesophyll conductance, and biochemistry, respectively. In the current study, the fitted photosynthetic parameters at $\psi_{leaf} = -0.3$ MPa were used as reference values. Thus,

$$\frac{dx}{x} \cong \frac{x_{0.3} - x}{x_{0.3}} \quad (15)$$

where x represents the fitted g_s, g_m, or J_f, (see Supplementary Table S1 for definitions of these and other mathematical parameters used in this paper), and $x_{0.3}$ represents the x value at $\psi_{leaf} = -0.3$ MPa.

Quantification of the contributions of hydraulic and hormonal signals to stomatal closure

The g_s model, originally presented by Buckley *et al.* (2003) and subsequently modified by Rodriguez-Dominguez *et al.* (2016), was used to examine the contributions of hydraulic and hormonal signals to the decline in g_s under drought. In this model, g_s is expressed as:

$$g_s = \frac{naK_{leaf}(\psi_{stem} + \pi)}{K_{leaf} + na\Delta w} \quad (16)$$

where π is bulk leaf osmotic pressure, Δw is the leaf-to-air water vapor mole fraction gradient, n represents the effect of hormonal signals on the sensitivity of guard cell osmotic pressure to leaf turgor, and a represents the relative adenosine triphosphate concentration. In this study, K_{leaf}, ψ_{stem}, Δw, and π were measured, a was simulated, and n was fitted. The π value was measured using a WP4C water potential meter (Decagon, Pullman, WA, USA).

Statistical analysis

Regressions were fitted with a linear model, and regression lines are shown when $P<0.05$. The correlations between the leaf functional traits (K_{leaf}, A, g_s, g_m, and J_f) and ψ_{leaf} were tested by four functions described in a previous study (Scoffoni *et al.*, 2012): a linear function ($K_{leaf} = a\psi_{leaf} + b$), a sigmoidal function ($K_{leaf} = \frac{a}{1+e^{-(\frac{\psi_{leaf}-x_0}{b})}}$), a logistic function ($K_{leaf} = \frac{a}{1+(\frac{\psi_{leaf}}{x_0})^b}$), and an exponential function ($K_{leaf} = \gamma_0 + a \cdot e^{-b \cdot \psi_{leaf}}$). The functions were compared using the Akaike Information Criterion (AIC) corrected for low n. The function with the lowest AIC value was chosen as the maximum likelihood function. The differences of K_{leaf} vulnerability among genotypes and methods were compared using a two-sample Kolmogorov–Smirnov test. All of the analyses were performed in the program R (R Core Team, 2018).

Results

Effects of 2 weeks of water stress on plant performance

The 2-week drought treatment led to a significant reduction in rice biomass (by 17.5% in CY1000 and 20.9% in YLY6; Fig. 1). Drought stress significantly increased LMA (by 13.8% in CY1000 and 15.5% in YLY6) and VLA (by 25.1% in CY1000 and 5.7% in YLY6), but decreased LA (by 14.1% in CY1000 and 15.0% in YLY6) and leaf width (LW) (by 10.8% in CY1000 and 9.3% in YLY6). VLA_{major} increased by 11.33% in CY1000 under water stress, but no changes were observed in YLY6; more pronounced increases in VLA_{minor} were observed for both genotypes (28.4% increase in CY1000 and 6.8% in YLY6).

Drought stress significantly decreased the gas exchange and leaf hydraulic traits in both rice genotypes, with more pronounced effects in YLY6 than CY1000 (Fig. 1). Overall, water stress decreased A, g_s, g_m, and K_{leaf} by 28.4%, 43.0%, 19.6%, and 50.2%, respectively. The leaf osmotic potential ($\psi_{osmotic}$)

Table 1. *Pressure–volume, gas exchange, and leaf hydraulic vulnerability parameters of rice*

Trait	CY1000	YLY6	Mean
SWC (g g^{-1})	2.31 ± 0.05	2.22 ± 0.06	2.27
π_0 (MPa)	−0.67 ± 0.14	−0.83 ± 0.11	−0.75
π_{tlp} (MPa)	−1.13 ± 0.12	−1.19 ± 0.06	−1.16
ε (MPa)	8.41 ± 2.10	6.96 ± 0.79	7.69
$K_{max\text{-}RKM}$ (mmol m^{-2} s^{-1} MPa^{-1})	8.02	9.25	8.47
$K_{max\text{-}EFM}$ (mmol m^{-2} s^{-1} MPa^{-1})	12.2	11.73	11.9
$K_{max\text{-}licor}$ (mmol m^{-2} s^{-1} MPa^{-1})	15.4	15.47	15.5
A_{max} (μmol CO_2 m^{-2} s^{-1})	18.6	20.23	19.3
g_{smax} (mol H_2O m^{-2} s^{-1})	0.29	0.33	0.31
g_{mmax} (mol CO_2 m^{-2} s^{-1})	0.13	0.15	0.14
$P_{50\text{-}RKM}$ (MPa)	−0.82	−0.85	−0.84
$P_{50\text{-}EFM}$ (MPa)	−0.91	−0.82	−0.87
$P_{50\text{-}licor}$ (MPa)	−0.64	−0.64	−0.64
$P_{50\text{-}A}$ (MPa)	−0.93	−1.01	−0.99
$P_{50\text{-}gs}$ (MPa)	−0.91	−0.94	−0.93
$P_{50\text{-}gm}$ (MPa)	−0.99	−1.05	−1.03
$P_{50\text{-}Jf}$ (MPa)	−1.99	−1.98	−1.99

See Supplementary Table S1 for definitions of the parameters.

increased by 30.2% in CY1000 and 21.0% in YLY6 following the 2-week drought treatment. In addition, water stress decreased g_{cut} in CY1000, but not in YLY6 (Fig. 1).

Leaf hydraulic and photosynthetic dynamics during short-term drought

The gas exchange and leaf hydraulic traits of rice were sensitive to short-term drought (Table 1; Figs 2 and 3). A, g_s, and g_m declined exponentially with decreasing ψ_{leaf}, with very similar patterns observed for the two genotypes (Fig. 2). Overall, the maximum A, g_s, and g_m values were 19.30 μmol CO_2 m^{-2} s^{-1}, 0.31 mol H_2O m^{-2} s^{-1}, and 0.14 mol CO_2 m^{-2} s^{-1}, respectively, with slightly higher values in YLY6 than CY1000. To quantify the sensitivity of the gas exchange traits to leaf drying, we estimated the leaf water potential values at 50% and 80% loss of function (P_{50} and P_{80}, respectively; Table 1; Fig. 2). The P_{50} values for A, g_s, and g_m were –0.99 MPa, –0.93 MPa, and

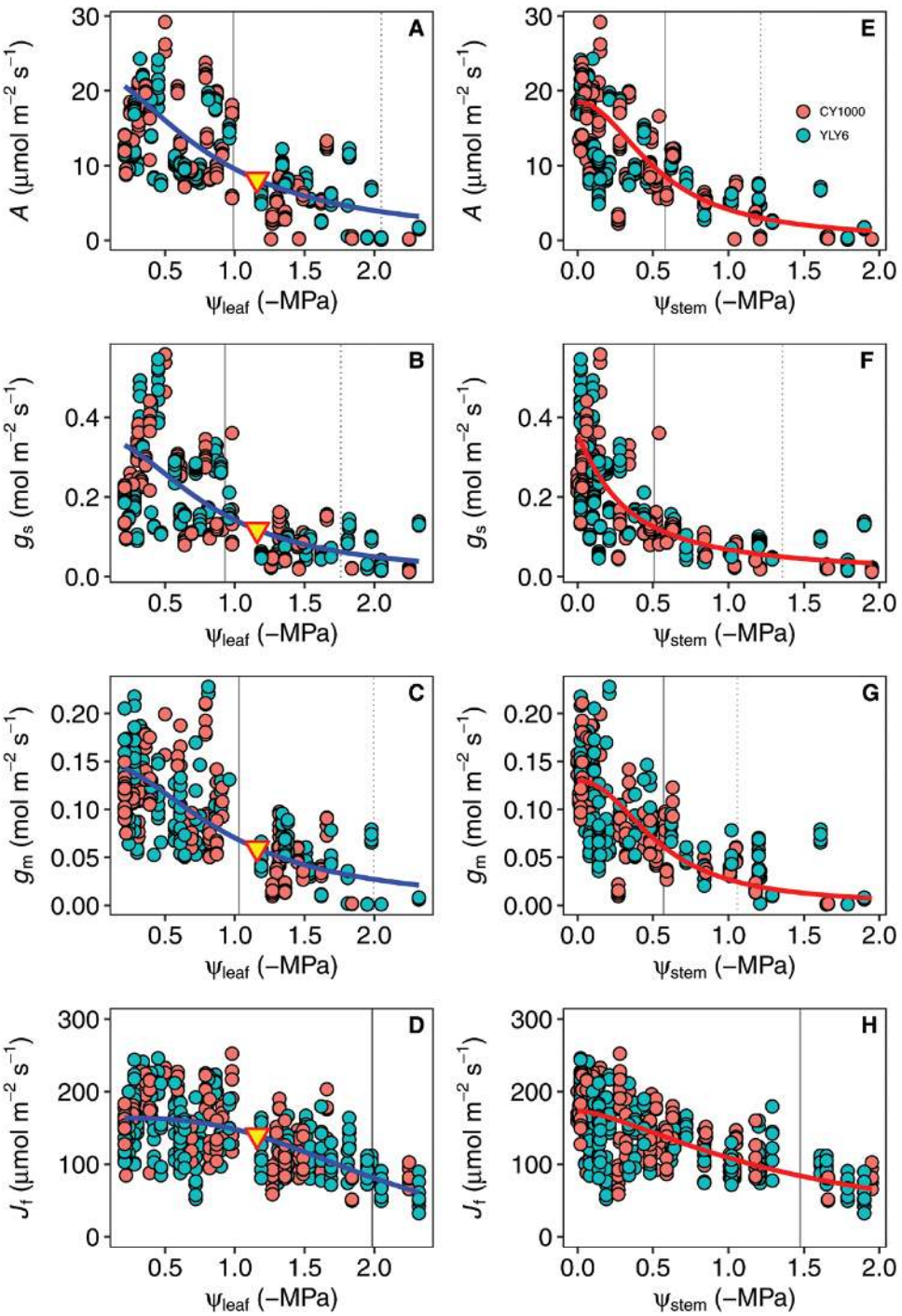

Fig. 2. Response of the gas exchange parameters to decreasing (A–D) leaf water potentials (ψ_{leaf}) and (E–H) stem water potentials (ψ_{stem}). The vertical solid and dotted lines indicate the water potential at 50% and 80% loss of function, respectively. The triangle represents the turgor loss point (Table 1). Fitted lines are the best-fit functions selected using maximum likelihood. (This figure is available in colour at *JXB* online.)

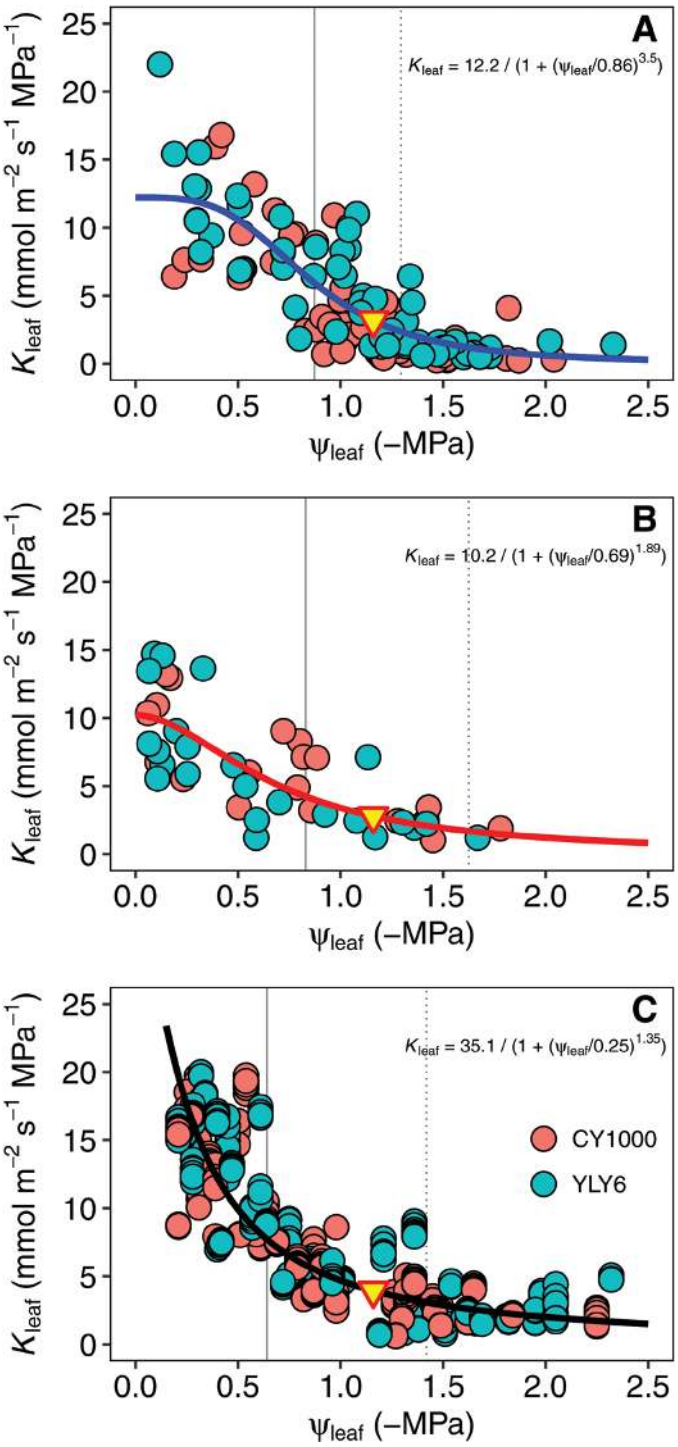

Fig. 3. Vulnerability of leaf hydraulic conductance (K_{leaf}) estimated by (A) the standard evaporative flux method (EFM), (B) the rehydration kinetic method, and (C) the gas exchange based EFM method. The vertical solid and dotted lines indicate the water potentials at 50% and 80% loss of K_{leaf}, respectively. The triangle represents the turgor loss point (Table 1). Fitted lines are the best-fit functions selected using maximum likelihood. (This figure is available in colour at *JXB* online.)

–1.03 MPa, respectively; however, the P_{50} of J_f was –1.99 MPa, which was lower than that of A.

K_{leaf} vulnerability curves were determined using three independent methods (Fig. 3). Although the curves of the two genotypes were indistinguishable when estimated with the same method (Supplementary Table S2), the curves estimated using the three methods were different (Supplementary Table S3). The maximum K_{leaf} from the gas exchange based EFM method was 15.5 mmol m^{-2} s^{-1} MPa^{-1}, almost twice as high as the 8.5 mmol m^{-2} s^{-1} MPa^{-1} estimated in the RKM method (Table 1). The P_{50} values of K_{leaf} were –0.84 MPa, –0.87 MPa, and –0.64 MPa for the RKM, EFM, and gas exchange based EFM methods, respectively. Moreover, the pressure–volume traits were similar in the two rice genotypes (Table 1), with average values for π_0, π_{tlp}, and ε of –0.75 MPa, –1.16 MPa, and 7.69 MPa, respectively.

Photosynthetic limitation analysis

Both g_s (r^2=0.78; P<0.001) and g_m (r^2=0.69; P<0.001) were tightly correlated with A during the drought treatment (Fig. 4A, B). Close correlations were also observed between K_{leaf} and g_s (r^2=0.39; P<0.001), and between K_{leaf} and g_m (r^2=0.31; P<0.001). The impacts of drought on the relative stomatal (l_s), mesophyll (l_m), and biochemical (l_b) limitations are shown in Fig. 5A. g_m was found to be the major limiting factor for photosynthesis in rice, as l_m contributed more than 40% of the relative limitation at any level of ψ_{leaf}. As ψ_{leaf} decreased in response to soil drought, both l_s and l_m increased; however, l_b declined dramatically. Diffusion processes appear to have a prominent role in limiting photosynthesis during soil drying (Fig. 5B), with diffusion through stomata (LS) and mesophyll (LM) having the greatest effect. Overall, the diffusion limitation (LM+LS) reached ~50% at a ψ_{leaf} of –1.0 MPa, while the contribution of biochemistry (LB) to the limitation of photosynthesis was very small.

We fitted the stomatal model to our data and then partitioned the observed declines in g_s into contributions from each variable in the model (Fig. 6). The turgor-independent parameter, n, declined dramatically with leaf dehydration, with a 4-fold decrease as the leaf water potential decreased from 0 to –1.5 MPa during soil drought. The a parameter was quite stable during leaf dehydration; however, the leaf osmotic pressure, π, increased exponentially under drought.

Discussion

In the present study, A declined under water stress, which resulted in a significant decrease in biomass accumulation. Photosynthesis in C_3 plants such as rice is limited by g_s, g_m, and/or the biochemistry of photosynthesis itself, including the enzymes and metabolites involved in the process as well as components of the thylakoid electron transport chain (Flexas, 2016). Our analysis showed that the total relative limitation of photosynthesis by g_s and g_m was greater than 80% in rice when the ψ_{leaf} dropped to –1.0 MPa following soil drying (Fig. 5A). The results of the present study, as well as those of previous studies (Flexas *et al.*, 2002; Galle *et al.*, 2011; Galmés *et al.*, 2013), highlight a major role for CO_2 diffusion in limiting A under conditions of water stress.

The decrease in g_s can be largely explained by K_{leaf} vulnerability under drought

We found that the g_s of rice declined with decreases in the stem (ψ_{stem}) and leaf (ψ_{leaf}) water potentials under drought

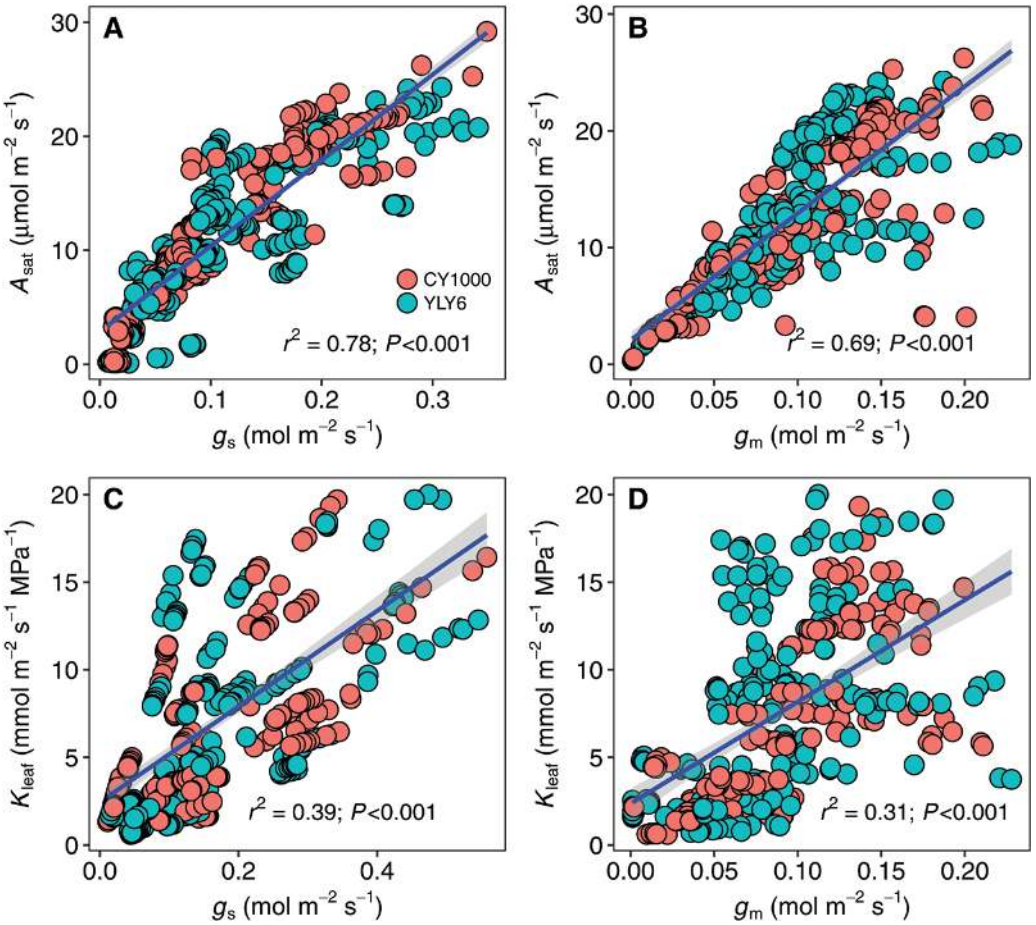

Fig. 4. (A, B) Relationships between light-saturated photosynthetic rate (*A*) and stomatal conductance (g_s) or mesophyll conductance to CO_2 (g_m). (C, D) Relationships between gas exchange based EFM estimation of leaf hydraulic conductance (K_{leaf}) and g_s or g_m. (This figure is available in colour at *JXB* online.)

conditions (Fig. 2). This decrease in g_s during soil drought has been widely studied, although the mechanisms for this response remain unclear. Two major mechanisms that regulate stomatal closure under drought conditions have been suggested to involve hydraulic (Sperry *et al.*, 2002; Buckley, 2005; Brodribb & Cochard, 2009; Rodriguez-Dominguez *et al.*, 2016) or hormonal (Dodd, 2005; McAdam *et al.*, 2016) processes. Although hormonal signals were not measured in the present study, we quantified the responses to the hormonal and hydraulic signals of drought by modeling them (Fig. 6). Consistent with the findings of Rodriguez-Dominguez *et al.* (2016), we demonstrated that stomatal closure during drought can be largely explained by hydraulic signals, although hormonal signals also play a role in decreasing g_s. Nevertheless, a recent study suggested that the drought-induced decline in K_{leaf} in isohydric grapevine (*Vitis vinifera*) genotypes is regulated by ABA accumulation (Coupel-Ledru *et al.*, 2017); thus, ABA could directly or indirectly regulate stomatal closure by decreasing K_{leaf}. Future studies are required to clarify the direct and indirect impacts of ABA on stomatal closure under soil drought conditions.

The mechanisms of K_{leaf} decline during dehydration are still largely unknown. K_{leaf} consists of at least two components, the conductance within the xylem (K_x) and the conductance through tissues outside the xylem (K_{ox}); therefore, the decline of K_{leaf} during dehydration could potentially be caused by changes in either or both of these factors. Increases in xylem tension during dehydration can cause air bubbles to form in the xylem conduit pit (Brodribb *et al.*, 2016*a*; Brodribb *et al.*, 2016*b*; Skelton *et al.*, 2017), which decrease K_x. When the tension in the xylem conduits exceeds the biomechanical resistance of the cell wall, the conduits collapse (Cochard *et al.*, 2004; Brodribb & Holbrook, 2005; Bouche *et al.*, 2016). K_x vulnerability cannot always fully explain the observed decline in K_{leaf}; for instance, K_{leaf} can decline early, at high ψ_{leaf}, before an embolism has been observed (Brodribb & Holbrook, 2006; Scoffoni *et al.*, 2012; Sack *et al.*, 2016). Indeed, some direct insights have challenged the major role for K_x vulnerability in driving K_{leaf} decline (Trifiló *et al.*, 2016; Scoffoni *et al.*, 2017*a*). In this study, we did not separate the contributions of K_x and K_{ox} to the decline in K_{leaf} during drought; however, Stiller *et al.* (2003) reported that the P_{50} of K_x in rice is approximately −2.0 MPa, which is far lower than that of the K_{leaf} observed here (Table 1), indicating that the decrease in K_{leaf} in rice during drought might be more closely connected to K_{ox} vulnerability. Water movement outside the xylem is complex and dynamic, involving apoplastic, symplastic, and transmembrane liquid flow paths and vapor diffusion within the intercellular airspaces (Buckley, 2015; Buckley

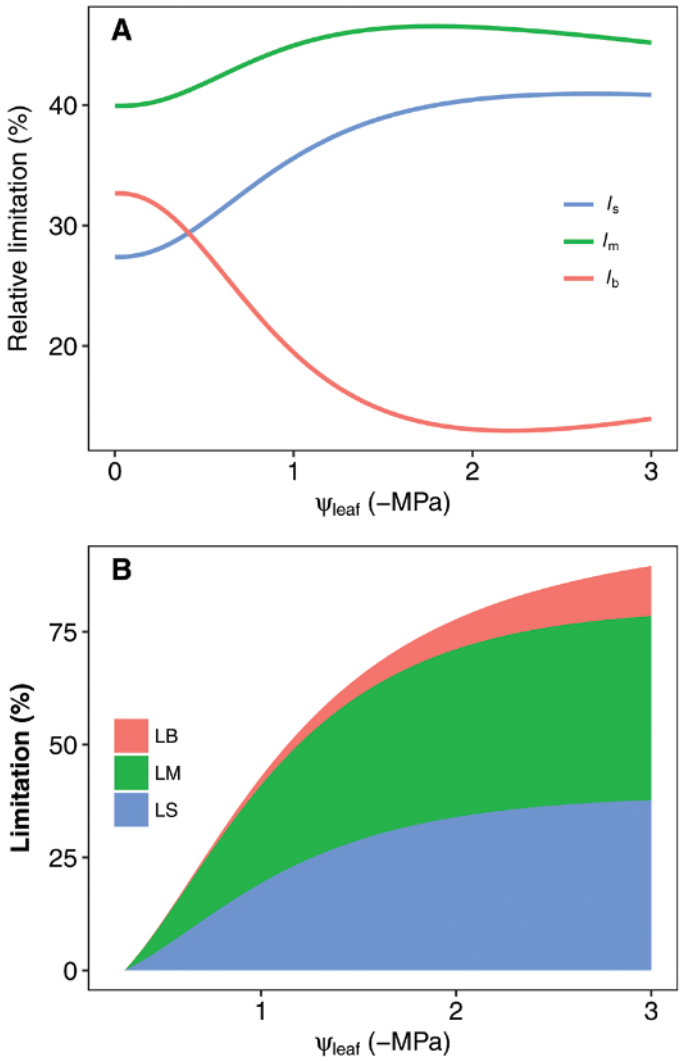

Fig. 5. Effects of leaf water potential (ψ_{leaf}) on (A) the distribution of the relative limits on photosynthesis caused by stomatal diffusion (l_s), mesophyll diffusion (l_m), and biochemistry (l_b), and (B) the overall ψ_{leaf}-dependent reduction in photosynthesis due to stomatal diffusion (LB), mesophyll diffusion (LM), and photosynthetic biochemistry (LB). (This figure is available in colour at *JXB* online.)

et al., 2015; Buckley *et al.*, 2017). During leaf dehydration, cells may be less well connected to each other owing to changes in their shape and size caused by leaf shrinkage. Indeed, the initial slope of the vulnerability curve, before the turgor loss point, has been suggested to be more related to decreases in K_{ox} than K_x (Scoffoni *et al.*, 2014; Hernandez-Santana *et al.*, 2016). In this study, K_{leaf} decreased sharply before π_{tlp}, suggesting that K_{ox} vulnerability played a major role in K_{leaf} decline. Moreover, the membrane permeability of the bundle sheath and mesophyll tissues has been suggested to influence K_{leaf}, and this effect may be related to the activities of aquaporins (Laur & Hacke, 2014; Sade *et al.*, 2014*b*).

Currently, all methods for estimating K_{leaf} have limitations (both common and specific to each method) that require consideration when interpreting data (Flexas *et al.*, 2013). As shown in Fig. 3, the K_{leaf} vulnerability curve of rice is method dependent, despite the similar values observed between genotypes for any given method. The K_{leaf} vulnerability curve produced using EFM has a similar shape to the one generated using RKM (see the equations in Fig. 3 and statistics in Supplementary Table S2); however, the EFM method shows a much higher maximum K_{leaf} (K_{max}; Table 1) value. Considering that the RKM measurement was performed in darkness, the difference may have been caused by light-dependent aquaporin activation (Cochard *et al.*, 2007; Scoffoni *et al.*, 2008). Indeed, we previously observed that rice K_{leaf} measured using EFM was strongly affected by light (Xiong *et al.*, 2018). In addition, the shape of the K_{leaf} vulnerability curve generated using the gas exchange based EFM method clearly differed from those produced using the other two methods, especially at high ψ_{leaf} values (>–0.5 MPa). One possible reason for these high K_{leaf} values at high ψ_{leaf} could be the imprecise method used to measure ψ_{stem}. Although the leaves were wrapped and equilibrated overnight in this study, ψ_{stem} is technically challenging to measure precisely using pressure chambers in leaves that are close to full hydration.

Responses of g_m to short-term soil drought

As reported for many species (Grassi & Magnani, 2005; Flexas *et al.*, 2006*a*; Warren, 2008; Flexas *et al.*, 2009; Galle *et al.*, 2009; Cano *et al.*, 2013), we observed that g_m in rice decreased with soil drought. Methodological problems exist in all currently available estimation techniques for g_m (Tholen *et al.*, 2012; Gu & Sun, 2014). One of the challenges for measuring g_m under drought conditions (low g_s) is the accurate estimation of C_i, because of the increasing relative contribution of g_{cut} to the overall leaf conductance, since the cuticular conductance for water is far greater than that for CO_2. In this study, we carefully ruled out the effects of g_{cut} on C_i. As it was not possible to estimate g_m under non-photorespiratory conditions using the variable J method, the effects of mitochondrial recycling of CO_2 on g_m were not estimated here; however, the 3-fold decrease in g_m observed in this study is unlikely to have been caused by (photo)respiration alone. We therefore assume that the decrease in g_m values observed during drought was mostly due to the decline of g_m *per se*.

The causes of the decrease in g_m during leaf dehydration are largely unknown, although g_m has been confirmed to be tightly correlated with mesophyll structure, membrane permeability, and the function of enzymes in the cytoplasm and chloroplast stroma (Flexas *et al.*, 2008; Evans *et al.*, 2009; Xiong *et al.*, 2015*a*; Xiong *et al.*, 2017). The two most important structural traits related to g_m are the cell wall thickness and the area of the chloroplast surface facing the intercellular airspace per unit leaf area (S_c; Evans *et al.*, 2009; Tosens *et al.*, 2012; Tomás *et al.*, 2013; Tosens *et al.*, 2016; Xiong *et al.*, 2017). S_c is related to the mesophyll cells themselves, as well as to the shape of chloroplasts and the light-dependent arrangement of chloroplasts (Tholen *et al.*, 2008). During leaf dehydration, the chloroplasts may move to reduce photodamage to the photosystems, and thus potentially change the values of S_c (Tholen *et al.*, 2008). As for water transport outside the xylem, the decline of membrane permeability, mediated by aquaporins, is suggested to correspond with the decrease in g_m (Flexas *et al.*, 2006*b*; Perez-Martin *et al.*, 2014; Sade

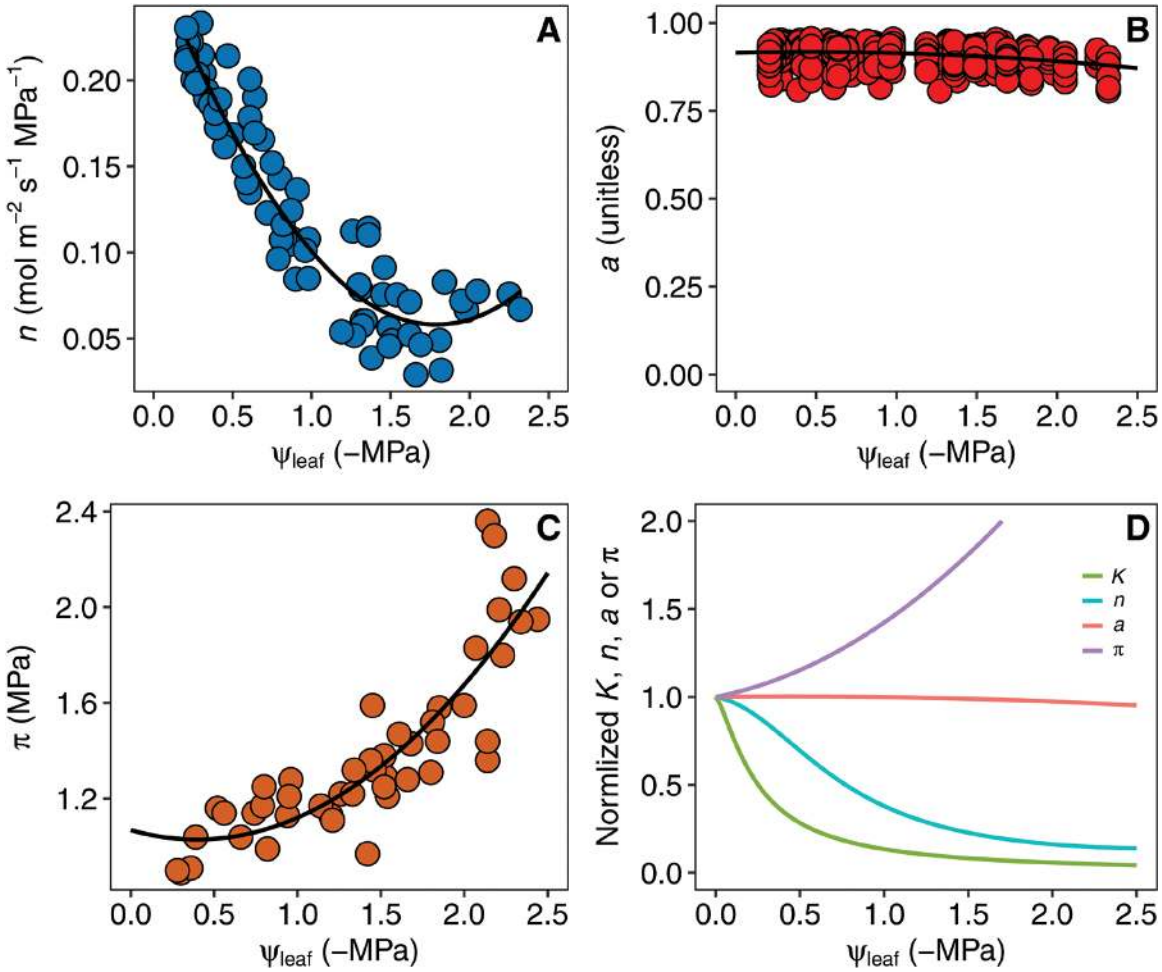

Fig. 6. Responses of variables in the stomatal model to changes in leaf water potential (ψ_{leaf}). (A) *n*, a turgor-independent parameter representing the effects of hormonal signals on the sensitivity of guard cell osmotic pressure to leaf turgor. (B) *a*, the relative concentration of adenosine triphosphate. (C) *π*, leaf osmotic pressure. (D) The parameters normalized by their values at a ψ_{leaf} of 0 MPa. *K*, gas exchange based EFM estimation of K_{leaf}, as in Fig. 3C. (This figure is available in colour at *JXB* online.)

et al., 2014*a*). The change in cell wall properties might be one of the reasons for the decline in g_m under drought, as water stress usually introduces changes in the bulk elastic modulus of the cell wall (Brodribb & Holbrook, 2003; Saito & Terashima, 2004; Guyot *et al.*, 2012), involving alteration of its biochemical composition and/or thickness. In addition, as shown in this study and previously (Théroux-Rancourt *et al.*, 2014; Théroux-Rancourt *et al.*, 2015), the K_{leaf}, A, g_s, and g_m vulnerability curves are almost always described as containing large measurement noise and/or high variability. Although estimation biases are inherently associated with all of the currently available techniques used to estimate K_{leaf} and g_m, the large number of different leaves used to construct the curves may be responsible for the major sources of variability. Hence, developing new methods to construct vulnerability curves based on a single leaf is perhaps one way to reduce the estimation variability in the future.

K_{leaf} vulnerability as a potential trigger for decline in g_s and g_m

Correlations between A, g_s, g_m, and K_{leaf} have been widely observed in many species, in part because of the common pathways for CO_2 diffusion and water transport within leaves, as well as between the leaf and atmosphere (Flexas *et al.*, 2013; Théroux-Rancourt *et al.*, 2015; Xiong *et al.*, 2015*b*; Xiong *et al.*, 2018). To determine whether these traits truly influence each other, these correlations would need to be observed for plants grown in the same conditions and measured under variable environmental conditions. As shown in Fig. 4, rice grown in the same environment and exposed to short-term changes in soil water content displayed a positive correlation between K_{leaf} and both g_s and g_m. Positive correlations between g_s and K_{leaf} across short-term environmental changes have been observed in many species (Théroux-Rancourt *et al.*, 2015; Gleason *et al.*, 2017; Xiong *et al.*, 2018); however, the positive correlation observed between g_m and K_{leaf} contradicts the findings of Loucos *et al.* (2017), who found no correlation between these traits in cotton (*Gossypium* sp.) measured under different light intensities. Although different species were used, the reason for this discrepancy is unclear. However, our results do support previous observations in grapevine (*Vitis* sp.) and poplar (*Populus* sp.) subjected to short-term soil drought (Ferrio *et al.*, 2012; Théroux-Rancourt *et al.*, 2014).

One of the novel findings of this study is the role of K_{leaf} vulnerability in triggering the decrease in g_s and g_m. In general, changes in A, g_s, and g_m in response to ψ_{leaf} were similar to the K_{leaf} vulnerability curves in rice; however, the P_{50} of K_{leaf} was higher than for g_s and g_m (Figs 2 and 3; Table 1). Our observations in rice disprove the previously proposed hypothesis, which suggested that stomata close early to reduce xylem tension and thus prevent plant hydraulic dysfunction (Cochard *et al.*, 2004; Brodribb & Holbrook, 2006; Hochberg *et al.*, 2017). As discussed above, K_{leaf} vulnerability might be largely determined by the non-xylem water movement pathways, and thus be influenced directly by the hydraulic effects that also trigger stomatal closure (Brodribb & Holbrook, 2003; Guyot *et al.*, 2012). Indeed, a recent study showed that stomatal closure under drought is induced by hydraulic signals but maintained by ABA (Tombesi *et al.*, 2015).Changes in hormone levels and/or leaf structural properties potentially decrease g_m. Interestingly, accumulation of ABA during drought conditions has been reported to decrease g_m significantly (Mizokami *et al.*, 2015); moreover, a slight increase in the leaf ABA level is enough to decrease g_s, but decreases in g_m require higher leaf levels of ABA (Mizokami *et al.*, 2015). The observation that g_s is more sensitive to drought than g_m may relate to the accumulation of ABA in leaves.

Modification of leaf anatomy facilitates the acclimation of leaf physiology to long-term drought

The acclimation of leaf anatomy and physiology to long-term drought was found to be coordinated in rice (Fig. 1). The LA and LW of the two rice genotypes displayed coordinated acclimation to drought, with the decrease in LA largely resulting from the narrowing of the leaf. Interestingly, a previous study found that grass species with naturally narrow leaves have high physiological drought tolerance (Craine *et al.*, 2012). The decrease in LW is also associated with an increase in leaf vein density, which could result from the declining LW and/or increasing vein numbers. For instance, a perfectly coordinated acclimation of vein density and LW would suggest that vein spacing is determined passively by differences in leaf expansion. In this study, the major vein (VLA_{major}) and minor vein densities(VLA_{minor}) increased to different degrees under drought, suggesting that the increased leaf vein density is regulated both passively and actively in rice (Fig. 1). Moreover, the genotype-dependent differences in leaf vein density changes under drought may underpin the different drought tolerances of the two genotypes studied. The acclimation of the physiological traits to long-term drought was genotype dependent, providing further evidence that modification of leaf vein density facilitates the physiological acclimation to drought in rice. Higher leaf vein densities in drought-acclimated leaves have a higher hydraulic capacity, and thus assimilate higher quantities of carbon. Vein density is closely related to K_{leaf} because greater vein densities, especially of the minor veins, are associated with higher K_{ox} and K_x values (Buckley *et al.*, 2015). In the present study, the responses of g_m and g_{cut} were also genotype dependent, suggesting that the mesophyll and epidermal tissues are also responsive to physiological acclimation in rice. However, we could not evaluate the effects of drought-induced anatomical and physiological changes on drought tolerance capacity because we did not construct pressure–volume curves and K_{leaf} vulnerability curves after drought treatment. Future research should focus on the effects of anatomical and physiological changes on drought tolerance.

In conclusion, these results provide new evidence that K_{leaf} and gas exchange are coordinated under drought conditions. Photosynthesis under drought conditions is primarily limited by g_s and g_m, and the decreased g_s was mainly determined by the decline in K_{leaf}, although it was also related to drought-induced hormonal signals. The decreased g_m and K_{leaf} are likely related to the changes in leaf anatomy and membrane permeability caused by drought.

Supplementary data

Supplementary data are available at *JXB* online.

Table S1. List of mathematical parameters and their units of measurement.

Table S2. Two-sample Kolmogorov-Smirnov test results in comparing K_{leaf} vulnerability of two rice genotypes.

Table S3. Two-sample Kolmogorov-Smirnov test results comparing K_{leaf} vulnerability methods.

Fig. S1. Climate information during the experiment (2017).

Acknowledgements

The authors thank Mr Zhuang Xiong for plants preparing and Dr Tom Buckley for helpful discussion. This work was partly supported by the National Key Program of R&D of China (No. 2016YFD0300210), the Program for Changjiang Scholars and Innovative Research Team in University of China (IRT1247), and the earmarked fund for China Agriculture Research System (CARS-01-20). DX was awarded by China Postdoctoral Science Foundation (2017M620326).

Author contributions

DX planned and designed the research; XW and TD performed the experiments; DX, XW, and TD analyzed the data and wrote the manuscript; all authors revised the manuscript.

References

Blackman CJ, Brodribb TJ. 2011. Two measures of leaf capacitance: insights into the water transport pathway and hydraulic conductance in leaves. Functional Plant Biology **38,** 118–126.

Bouche PS, Delzon S, Choat B, *et al*. 2016. Are needles of *Pinus pinaster* more vulnerable to xylem embolism than branches? New insights from X-ray computed tomography. Plant, Cell & Environment **39,** 860–870.

Boyer JS. 2015a. Impact of cuticle on calculations of the CO_2 concentration inside leaves. Planta **242,** 1405–1412.

Boyer JS. 2015b. Turgor and the transport of CO_2 and water across the cuticle (epidermis) of leaves. Journal of Experimental Botany **66,** 2625–2633.

Boyer JS, Wong SC, Farquhar GD. 1997. CO_2 and water vapor exchange across leaf cuticle (epidermis) at various water potentials. Plant Physiology **114,** 185–191.

Brodribb TJ, Bienaimé D, Marmottant P. 2016a. Revealing catastrophic failure of leaf networks under stress. Proceedings of the National Academy of Sciences, USA **113,** 4865–4869.

Brodribb TJ, Cochard H. 2009. Hydraulic failure defines the recovery and point of death in water-stressed conifers. Plant Physiology **149,** 575–584.

Brodribb TJ, Feild TS, Jordan GJ. 2007. Leaf maximum photosynthetic rate and venation are linked by hydraulics. Plant Physiology **144,** 1890–1898.

Brodribb TJ, Holbrook NM. 2003. Stomatal closure during leaf dehydration, correlation with other leaf physiological traits. Plant Physiology **132,** 2166–2173.

Brodribb TJ, Holbrook NM. 2005. Water stress deforms tracheids peripheral to the leaf vein of a tropical conifer. Plant Physiology **137,** 1139–1146.

Brodribb TJ, Holbrook NM. 2006. Declining hydraulic efficiency as transpiring leaves desiccate: two types of response. Plant, Cell & Environment **29,** 2205–2215.

Brodribb TJ, Holbrook NM, Zwieniecki MA, Palma B. 2005. Leaf hydraulic capacity in ferns, conifers and angiosperms: impacts on photosynthetic maxima. New Phytologist **165,** 839–846.

Brodribb TJ, Skelton RP, McAdam SA, Bienaimé D, Lucani CJ, Marmottant P. 2016b. Visual quantification of embolism reveals leaf vulnerability to hydraulic failure. New Phytologist **209,** 1403–1409.

Buckley TN. 2005. The control of stomata by water balance. New Phytologist **168,** 275–292.

Buckley TN. 2015. The contributions of apoplastic, symplastic and gas phase pathways for water transport outside the bundle sheath in leaves. Plant, Cell & Environment **38,** 7–22.

Buckley TN, Diaz-Espejo A. 2015. Partitioning changes in photosynthetic rate into contributions from different variables. Plant, Cell & Environment **38,** 1200–1211.

Buckley TN, John GP, Scoffoni C, Sack L. 2015. How does leaf anatomy influence water transport outside the xylem? Plant Physiology **168,** 1616–1635.

Buckley TN, John GP, Scoffoni C, Sack L. 2017. The sites of evaporation within leaves. Plant Physiology **173,** 1763–1782.

Buckley TN, Mott KA, Farquhar GD. 2003. A hydromechanical and biochemical model of stomatal conductance. Plant, Cell & Environment **26,** 1767–1785.

Cano FJ, Sánchez-Gómez D, Rodríguez-Calcerrada J, Warren CR, Gil L, Aranda I. 2013. Effects of drought on mesophyll conductance and photosynthetic limitations at different tree canopy layers. Plant, Cell & Environment **36,** 1961–1980.

Cochard H, Froux F, Mayr S, Coutand C. 2004. Xylem wall collapse in water-stressed pine needles. Plant Physiology **134,** 401–408.

Cochard H, Venisse JS, Barigah TS, Brunel N, Herbette S, Guilliot A, Tyree MT, Sakr S. 2007. Putative role of aquaporins in variable hydraulic conductance of leaves in response to light. Plant Physiology **143,** 122–133.

Coupel-Ledru A, Tyerman SD, Masclef D, Lebon E, Christophe A, Edwards EJ, Simonneau T. 2017. Abscisic acid down-regulates hydraulic conductance of grapevine leaves in isohydric genotypes only. Plant Physiology **175,** 1121–1134.

Craine JM, Ocheltree TW, Nippert JB, Towne EG, Skibbe AM, Kembel SW, Fargione JE. 2012. Global diversity of drought tolerance and grassland climate-change resilience. Nature Climate Change **3,** 63–67.

Dodd IC. 2005. Root-to-shoot signalling: assessing the roles of 'up' in the up and down world of long-distance signalling *in planta*. Plant and Soil **274,** 251–270.

Evans JR, Kaldenhoff R, Genty B, Terashima I. 2009. Resistances along the CO_2 diffusion pathway inside leaves. Journal of Experimental Botany **60,** 2235–2248.

Ferrio JP, Pou A, Florez-Sarasa I, Gessler A, Kodama N, Flexas J, Ribas-Carbó M. 2012. The Péclet effect on leaf water enrichment correlates with leaf hydraulic conductance and mesophyll conductance for CO_2. Plant, Cell & Environment **35,** 611–625.

Flexas J. 2016. Genetic improvement of leaf photosynthesis and intrinsic water use efficiency in C_3 plants: why so much little success? Plant Science **251,** 155–161.

Flexas J, Barbour MM, Brendel O, *et al*. 2012. Mesophyll diffusion conductance to CO_2: an unappreciated central player in photosynthesis. Plant Science **193–194,** 70–84.

Flexas J, Barón M, Bota J, *et al*. 2009. Photosynthesis limitations during water stress acclimation and recovery in the drought-adapted *Vitis* hybrid Richter-110 (*V. berlandieri*×*V. rupestris*). Journal of Experimental Botany **60,** 2361–2377.

Flexas J, Bota J, Escalona JM, Sampol B, Medrano H. 2002. Effects of drought on photosynthesis in grapevines under field conditions an evaluation of stomatal and mesophyll limitations. Functional Plant Biology **29,** 461–471.

Flexas J, Ribas-Carbó M, Bota J, Galmés J, Henkle M, Martínez-Cañellas S, Medrano H. 2006a. Decreased Rubisco activity during water stress is not induced by decreased relative water content but related to conditions of low stomatal conductance and chloroplast CO_2 concentration. New Phytologist **172,** 73–82.

Flexas J, Ribas-Carbó M, Diaz-Espejo A, Galmés J, Medrano H. 2008. Mesophyll conductance to CO_2: current knowledge and future prospects. Plant, Cell & Environment **31,** 602–621.

Flexas J, Ribas-Carbó M, Hanson DT, Bota J, Otto B, Cifre J, McDowell N, Medrano H, Kaldenhoff R. 2006b. Tobacco aquaporin NtAQP1 is involved in mesophyll conductance to CO_2 *in vivo*. The Plant Journal **48,** 427–439.

Flexas J, Scoffoni C, Gago J, Sack L. 2013. Leaf mesophyll conductance and leaf hydraulic conductance: an introduction to their measurement and coordination. Journal of Experimental Botany **64,** 3965–3981.

Galle A, Florez-Sarasa I, Aououad HE, Flexas J. 2011. The Mediterranean evergreen *Quercus ilex* and the semi-deciduous *Cistus albidus* differ in their leaf gas exchange regulation and acclimation to repeated drought and re-watering cycles. Journal of Experimental Botany **62,** 5207–5216.

Galle A, Florez-Sarasa I, Tomas M, Pou A, Medrano H, Ribas-Carbo M, Flexas J. 2009. The role of mesophyll conductance during water stress and recovery in tobacco (*Nicotiana sylvestris*): acclimation or limitation? Journal of Experimental Botany **60,** 2379–2390.

Galmés J, Molins A, Flexas J, Conesa MÀ. 2017. Coordination between leaf CO_2 diffusion and Rubisco properties allows maximizing photosynthetic efficiency in *Limonium* species. Plant, Cell & Environment **40,** 2081–2094.

Galmés J, Ochogavía JM, Gago J, Roldán EJ, Cifre J, Conesa MÀ. 2013. Leaf responses to drought stress in Mediterranean accessions of *Solanum lycopersicum*: anatomical adaptations in relation to gas exchange parameters. Plant, Cell & Environment **36,** 920–935.

Gleason SM, Wiggans DR, Bliss CA, Comas LH, Cooper M, DeJonge KC, Young JS, Zhang H. 2017. Coordinated decline in photosynthesis and hydraulic conductance during drought stress in *Zea mays*. Flora **227,** 1–9.

Grassi G, Magnani F. 2005. Stomatal, mesophyll conductance and biochemical limitations to photosynthesis as affected by drought and leaf ontogeny in ash and oak trees. Plant, Cell & Environment **28,** 834–849.

Gu L, Sun Y. 2014. Artefactual responses of mesophyll conductance to CO_2 and irradiance estimated with the variable *J* and online isotope discrimination methods. Plant, Cell & Environment **37,** 1231–1249.

Guyot G, Scoffoni C, Sack L. 2012. Combined impacts of irradiance and dehydration on leaf hydraulic conductance: insights into vulnerability and stomatal control. Plant, Cell & Environment **35,** 857–871.

Hanson DT, Stutz SS, Boyer JS. 2016. Why small fluxes matter: the case and approaches for improving measurements of photosynthesis and (photo)respiration. Journal of Experimental Botany **67,** 3027–3039.

Harley PC, Loreto F, Di Marco G, Sharkey TD. 1992. Theoretical considerations when estimating the mesophyll conductance to CO_2 flux by analysis of the response of photosynthesis to CO_2. Plant Physiology **98,** 1429–1436.

Hermida-Carrera C, Kapralov MV, Galmés J. 2016. Rubisco catalytic properties and temperature response in crops. Plant Physiology **171,** 2549–2561.

Hernandez-Santana V, Rodriguez-Dominguez CM, Fernández JE, Diaz-Espejo A. 2016. Role of leaf hydraulic conductance in the regulation of stomatal conductance in almond and olive in response to water stress. Tree Physiology **36,** 725–735.

Hochberg U, Windt CW, Ponomarenko A, Zhang YJ, Gersony J, Rockwell FE, Holbrook NM. 2017. Stomatal closure, basal leaf embolism, and shedding protect the hydraulic integrity of grape stems. Plant Physiology **174,** 764–775.

Holbrook NM, Shashidhar VR, James RA, Munns R. 2002. Stomatal control in tomato with ABA-deficient roots: response of grafted plants to soil drying. Journal of Experimental Botany **53,** 1503–1514.

Laur J, Hacke UG. 2014. The role of water channel proteins in facilitating recovery of leaf hydraulic conductance from water stress in *Populus trichocarpa*. PLoS One **9,** e111751.

Loucos KE, Simonin KA, Barbour MM. 2017. Leaf hydraulic conductance and mesophyll conductance are not closely related within a single species. Plant, Cell & Environment **40,** 203–215.

Martínez-Vilalta J, Garcia-Forner N. 2017. Water potential regulation, stomatal behaviour and hydraulic transport under drought: deconstructing the iso/anisohydric concept. Plant, Cell & Environment **40,** 962–976.

McAdam SA, Brodribb TJ. 2016. Linking turgor with ABA biosynthesis: implications for stomatal responses to vapor pressure deficit across land plants. Plant Physiology **171,** 2008–2016.

McAdam SA, Sussmilch FC, Brodribb TJ. 2016. Stomatal responses to vapour pressure deficit are regulated by high speed gene expression in angiosperms. Plant, Cell & Environment **39,** 485–491.

Mizokami Y, Noguchi K, Kojima M, Sakakibara H, Terashima I. 2015. Mesophyll conductance decreases in the wild type but not in an ABA-deficient mutant (*aba1*) of *Nicotiana plumbaginifolia* under drought conditions. Plant, Cell & Environment **38,** 388–398.

Perez-Martin A, Michelazzo C, Torres-Ruiz JM, Flexas J, Fernández JE, Sebastiani L, Diaz-Espejo A. 2014. Regulation of photosynthesis and stomatal and mesophyll conductance under water stress and recovery in olive trees: correlation with gene expression of carbonic anhydrase and aquaporins. Journal of Experimental Botany **65,** 3143–3156.

R Core Team. 2018. R: A language and environment for statistical computing. Vienna: The R Foundation for Statistical Computing. https://www.R-project.org/.

Rodriguez-Dominguez CM, Buckley TN, Egea G, de Cires A, Hernandez-Santana V, Martorell S, Diaz-Espejo A. 2016. Most stomatal closure in woody species under moderate drought can be explained by stomatal responses to leaf turgor. Plant, Cell & Environment **39,** 2014–2026.

Sack L, Buckley TN, Scoffoni C. 2016. Why are leaves hydraulically vulnerable? Journal of Experimental Botany **67,** 4917–4919.

Sack L, Cowan PD, Jaikumar N, Holbrook NM. 2003. The 'hydrology' of leaves: co-ordination of structure and function in temperate woody species. Plant, Cell & Environment **26,** 1343–1356.

Sack L, John GP, Buckley TN. 2018. ABA accumulation in dehydrating leaves is associated with decline in cell volume, not turgor pressure. Plant Physiology **176,** 489–495.

Sack L, Scoffoni C. 2011. Minimum epidermal conductance (g_{min}, a.k.a. cuticular conductance). PrometheusWiki. http://prometheuswiki.org/tiki-pagehistory.php?page=Minimum epidermal conductance (gmin, a.k.a. cuticular conductance)&preview=7.

Sade N, Gallé A, Flexas J, Lerner S, Peleg G, Yaaran A, Moshelion M. 2014a. Differential tissue-specific expression of *NtAQP1* in *Arabidopsis thaliana* reveals a role for this protein in stomatal and mesophyll conductance of CO_2 under standard and salt-stress conditions. Planta **239,** 357–366.

Sade N, Shatil-Cohen A, Attia Z, Maurel C, Boursiac Y, Kelly G, Granot D, Yaaran A, Lerner S, Moshelion M. 2014b. The role of plasma membrane aquaporins in regulating the bundle sheath-mesophyll continuum and leaf hydraulics. Plant Physiology **166,** 1609–1620.

Saito T, Terashima I. 2004. Reversible decreases in the bulk elastic modulus of mature leaves of deciduous *Quercus* species subjected to two drought treatments. Plant, Cell & Environment **27,** 863–875.

Scoffoni C, Albuquerque C, Brodersen CR, Townes SV, John GP, Bartlett MK, Buckley TN, McElrone AJ, Sack L. 2017a. Outside-xylem vulnerability, not xylem embolism, controls leaf hydraulic decline during dehydration. Plant Physiology **173,** 1197–1210.

Scoffoni C, McKown AD, Rawls M, Sack L. 2012. Dynamics of leaf hydraulic conductance with water status: quantification and analysis of species differences under steady state. Journal of Experimental Botany **63,** 643–658.

Scoffoni C, Pou A, Aasamaa K, Sack L. 2008. The rapid light response of leaf hydraulic conductance: new evidence from two experimental methods. Plant, Cell & Environment **31,** 1803–1812.

Scoffoni C, Rawls M, McKown A, Cochard H, Sack L. 2011. Decline of leaf hydraulic conductance with dehydration: relationship to leaf size and venation architecture. Plant Physiology **156,** 832–843.

Scoffoni C, Sack L, Ort D. 2017b. The causes and consequences of leaf hydraulic decline with dehydration. Journal of Experimental Botany **68,** 4479–4496.

Scoffoni C, Vuong C, Diep S, Cochard H, Sack L. 2014. Leaf shrinkage with dehydration: coordination with hydraulic vulnerability and drought tolerance. Plant Physiology **164,** 1772–1788.

Skelton RP, Brodribb TJ, Choat B. 2017. Casting light on xylem vulnerability in an herbaceous species reveals a lack of segmentation. New Phytologist **214,** 561–569.

Sperry JS, Hacke UG, Oren R, Comstock JP. 2002. Water deficits and hydraulic limits to leaf water supply. Plant, Cell & Environment **25,** 251–263.

Stiller V, Lafitte HR, Sperry JS. 2003. Hydraulic properties of rice and the response of gas exchange to water stress. Plant Physiology **132,** 1698–1706.

Théroux-Rancourt G, Éthier G, Pepin S. 2014. Threshold response of mesophyll CO_2 conductance to leaf hydraulics in highly transpiring hybrid poplar clones exposed to soil drying. Journal of Experimental Botany **65,** 741–753.

Théroux Rancourt G, Éthier G, Pepin S. 2015. Greater efficiency of water use in poplar clones having a delayed response of mesophyll conductance to drought. Tree Physiology **35,** 172–184.

Tholen D, Boom C, Noguchi K, Ueda S, Katase T, Terashima I. 2008. The chloroplast avoidance response decreases internal conductance to CO_2 diffusion in *Arabidopsis thaliana* leaves. Plant, Cell & Environment **31,** 1688–1700.

Tholen D, Ethier G, Genty B, Pepin S, Zhu XG. 2012. Variable mesophyll conductance revisited: theoretical background and experimental implications. Plant, Cell & Environment **35,** 2087–2103.

Tomás M, Flexas J, Copolovici L, Galmés J, Hallik L, Medrano H, Ribas-Carbó M, Tosens T, Vislap V, Niinemets Ü. 2013. Importance of leaf anatomy in determining mesophyll diffusion conductance to CO_2 across species: quantitative limitations and scaling up by models. Journal of Experimental Botany **64,** 2269–2281.

Tombesi S, Nardini A, Frioni T, Soccolini M, Zadra C, Farinelli D, Poni S, Palliotti A. 2015. Stomatal closure is induced by hydraulic signals and maintained by ABA in drought-stressed grapevine. Scientific Reports **5,** 12449.

Tosens T, Niinemets Ü, Westoby M, Wright IJ. 2012. Anatomical basis of variation in mesophyll resistance in eastern Australian sclerophylls: news of a long and winding path. Journal of Experimental Botany **63,** 5105–5119.

Tosens T, Nishida K, Gago J, *et al*. 2016. The photosynthetic capacity in 35 ferns and fern allies: mesophyll CO_2 diffusion as a key trait. New Phytologist **209,** 1576–1590.

Trenberth KE, Dai A, van der Schrier G, Jones PD, Barichivich J, Briffa KR, Sheffield J. 2013. Global warming and changes in drought. Nature Climate Change **4,** 17.

Trifiló P, Raimondo F, Savi T, Lo Gullo MA, Nardini A. 2016. The contribution of vascular and extra-vascular water pathways to drought-induced decline of leaf hydraulic conductance. Journal of Experimental Botany **67,** 5029–5039.

Valentini R, Epron D, De Angelis P, Matteucci G, Dreyer E. 1995. *In situ* estimation of net CO_2 assimilation, photosynthetic electron flow and photorespiration in *Turkey oak* (*Q. cerris* L.) leaves: diurnal cycles under different levels of water supply. Plant, Cell & Environment **18,** 631–640.

Veromann-Jürgenson LL, Tosens T, Laanisto L, Niinemets Ü. 2017. Extremely thick cell walls and low mesophyll conductance: welcome to the world of ancient living! Journal of Experimental Botany **68,** 1639–1653.

Wang X, Wang W, Huang J, Peng S, Xiong D. 2018. Diffusional conductance to CO_2 is the key limitation to photosynthesis in salt-stressed leaves of rice (*Oryza sativa*). Physiologia Plantarum **163,** 45–58.

Warren CR. 2008. Soil water deficits decrease the internal conductance to CO_2 transfer but atmospheric water deficits do not. Journal of Experimental Botany **59,** 327–334.

Xiong D, Douthe C, Flexas J. 2018. Differential coordination of stomatal conductance, mesophyll conductance, and leaf hydraulic conductance in response to changing light across species. Plant, Cell & Environment **41,** 436–450.

Xiong D, Flexas J, Yu T, Peng S, Huang J. 2017. Leaf anatomy mediates coordination of leaf hydraulic conductance and mesophyll conductance to CO_2 in *Oryza*. New Phytologist **213,** 572–583.

Xiong D, Liu X, Liu L, Douthe C, Li Y, Peng S, Huang J. 2015a. Rapid responses of mesophyll conductance to changes of CO_2 concentration, temperature and irradiance are affected by N supplements in rice. Plant, Cell & Environment **38,** 2541–2550.

Xiong D, Yu T, Zhang T, Li Y, Peng S, Huang J. 2015b. Leaf hydraulic conductance is coordinated with leaf morpho-anatomical traits and nitrogen status in the genus *Oryza*. Journal of Experimental Botany **66,** 741–748.

Zhang FP, Sussmilch F, Nichols DS, Cardoso AA, Brodribb TJ, McAdam SAM. 2018. Leaves, not roots or floral tissue, are the main site of rapid, external pressure-induced ABA biosynthesis in angiosperms. Journal of Experimental Botany **69,** 1261–1267.